



Gb/s Underwater Wireless Optical Communications Using Series-Connected GaN Micro-LED Arrays

B.V.Sai Koushik

GMR Institute of Technology Rajam, Andhra Pradesh India,532127
20341A0420@gmrit.edu.in

ABSTRACT

For many industrial and scientific underwater applications, high-speed wireless communications are very desirable. While radio frequency communications are severely constrained by attenuation in seawater, acoustic communications are plagued by excessive latency and low data rates. With high transmission speeds (up to Gb/s) and relatively low attenuation at visible wavelengths, optical communications are a possible replacement. Here, we use series-connected micro-light-emitting-diode (LED) arrays with six LED pixels that are either 60 or 80 mm in diameter and operate at 450 nm to show their utilisation. These innovations boost output power while preserving a comparatively high modulation bandwidth. We demonstrate underwater wireless data transmission using orthogonal frequency division multiplexing (OFDM) at rates of up to 4.92 Gb/s, 3.22 Gb/s, and 3.4 Gb/s over 1.5 m, 3 m, and 4.5 m, respectively, with corresponding bit error ratios (BERs) of $1.5 \cdot 10^3$, $1.1 \cdot 10^3$, and $3.1 \cdot 10^3$, through clear tap water, and Mb/s rates through >5 attenuation.

Search terms: GaN, miniature LED arrays, murky water, and wireless optical communications underwater.

INTRODUCTION

The control, monitoring, and maintenance of subsea infrastructure, as well as many other industrial, military, and scientific subsea activities, such as oceanographic surveying, necessitate the transfer of escalating vast amounts of data via high-speed communications. For applications like evaluating subsea oil and gas infrastructure, unmanned and autonomous underwater vehicles (UUVs and AUVs) are employed to acquire high-resolution photos or films. In this illustration, the image and video data that was collected would need to be sent back to a surface vessel for analysis, and the vehicles would also need to receive navigational directions and instructions. While underwater

cables or tethers can be used to provide high-speed data links, the harsh underwater environment might make this impossible, expensive, or in some situations, limiting. High-speed underwater wireless networks are therefore highly desired. Due to its long-range capabilities, which may reach lengths of up to tens of kilometres, acoustic technologies are the most popular type of underwater wireless communications. However, due to their constrained capacity, they only provide low data speeds (on the order of kb/s) (around tens of kHz). Additionally, the low speed and multipath propagation problems in acoustics can result in inter-symbol interference (ISI). Despite being

widely used in free space (e.g., in cell phones, TV, radio, and satellite communications), radio frequency (RF) communications are not easily deployable underwater because seawater significantly attenuates electromagnetic (EM) waves at these frequencies. As a result, underwater RF wireless communications are only capable of short distances and require large transmission powers and complicated antenna designs. Since water attenuates light most dramatically in the visible spectrum, underwater wireless optical communication (UWOC) may be a viable alternative to acoustics and RF. The rapid development of solid-state photoreceivers such single-photon avalanche diodes as well as efficient, compact, and resilient solid-state transmitters that emit light in the violet-blue-green area of the visible spectrum has also occurred over the past 20 years. As a result, visible wavelength-based high-speed underwater optical data transfer over tens of metres is now practicable. For instance, recent findings by Li et al. demonstrated 25 Gb/s over a 5 m distance using a vertical-cavity surface-emitting laser (VCSEL) operating at 680 nm. While Kong et al. used an RGB (Red, Green, and Blue) laser, Fei et al. demonstrated 16.6 Gb/s for 5 m and 6.6 Gb/s over 55 m of clear tap water.

uLED DESIGN

The blue-emitting III-nitride LED wafers used in the fabrication of the LED devices described here were grown on a 2" sapphire c-plane substrate with regularly patterned surfaces. The fabrication process is comparable to that explained in [15] and [16], and is outlined in the following manner. In order to define disk-shaped LED pixels, the n-GaN layer was etched down to using conventional photolithography and etching methods. With a 70 m distance between adjacent mesas, a further processing step etched down to the sapphire substrate to electrically-isolate each of these LEDs on individual 140 x 140 m² mesas (Fig. 1(a)). The LEDs were then connected in series by the deposition of P-type and N-type contact metals (Pd and Ti/Au). The series-connected LED array's simplified cross-sectional construction is depicted in Fig. 1(b), where two adjacent LED elements are used as an example, with the electrical connections between them underlined. The centre wavelength of all the devices is roughly 450 nm, and each of the LED pixels is either 60 or 80 mm in diameter. Each device, as depicted in Fig. 1(a), is made up of six LED pixels organised in a 3 by 2 array. To maximise the output power in this work, all 6 pixels were simultaneously driven in series. For the devices with 60 mm and 80 mm pixels that are connected in series. This displays the 3 dB electrical-to-electrical (E-E) and electrical-to-optical (E-O) bandwidths versus current characteristics, whereas this displays the current versus voltage (I-V) and the output optical power versus current (L-I). The forward detected output, known as optical power, was quantified by positioning the LEDs close to a Si photodiode that had been calibrated. The bandwidths were assessed as previously described. As demonstrated, the turn-on voltage for the 60 m

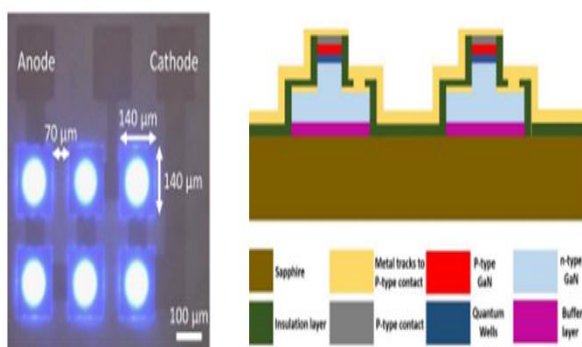


Fig 1: Manufacturing the uled

device at 1 mA is 21.7 V, or approximately 3.6 V for each LED element, whereas the turn-on voltage for the 80 m device is 20 V, or approximately 3.3 V for each LED element. Both devices can operate at currents greater than 50 mA and show optical power before thermal rollover of over 21 mW and 15 mW for the 80 m and 60 m respectively.

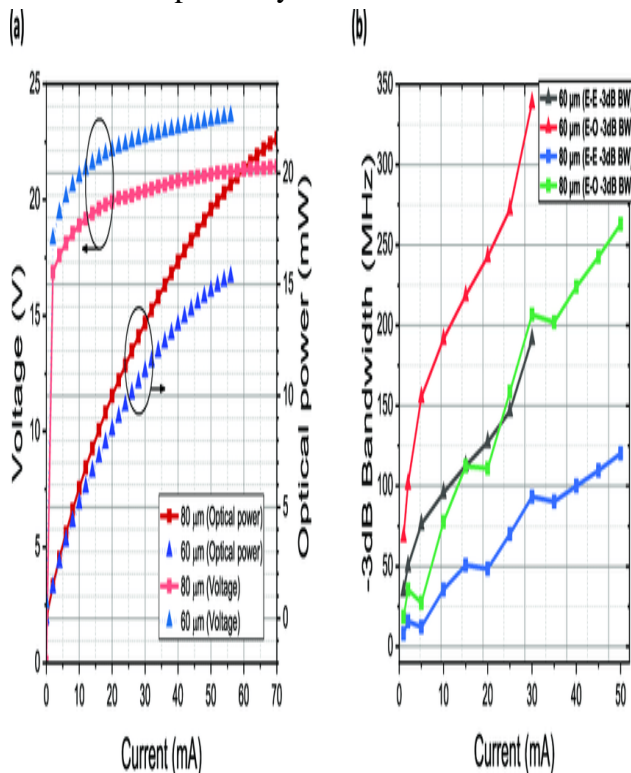


Fig 2: Voltage vs Current vs Optical Power

LITERATURE SURVEY

Paper 1

It is suggested and practically demonstrated to use a 25-Gbps underwater wireless optical communication (UWOC) system with a laser beam expander to increase the collimated beam diameter over a 5-m highly turbid harbour water link and a two-stage injection-locked 680-nm red-light vertical-cavity surface-emitting laser (VCSEL) transmitter to improve the

frequency response. This proposed 5 m/25 Gbps UWOC system uses a 680-nm red-light VCSEL transmitter rather than a 520-nm green-light LD transmitter or a 450-nm blue-light LD transmitter because the overall attenuation coefficient at 680 nm is smaller in highly turbid harbour water link than that at 520 and 450 nm. Real-time acquisition of a clear eye diagram and an acceptable bit error rate performance (3×10^{-9}). This proposed UWOC system with a two-stage injection-locked 680-nm VCSEL transmitter and a laser beam expander brings important improvements in the scenario characterized by high turbidity

Paper 2

Using III-nitride light-emitting diodes (LEDs) for visible light communication (VLC) has many benefits, including license-free operation, great spatial diversity, and inherent security. Micro-LEDs (LEDs) in particular are excellent VLC candidates because of their large modulation bandwidths. The performance of VLC is, however, significantly constrained by the modest optical power of a single LED. We describe an improved series-biased LED array in this study that increases optical power while maintaining a high modulation bandwidth for high-speed VLC. We offer a sample array of three LED elements with a diameter of 340 μm. A blue-emitting series-biased LED array's optical power and small signal 6-dB electrical modulation bandwidth are over 18.0 mW and 285 MHz, respectively, at a current density of 3200 A/cm² in direct-current operation. The ON-OFF keying, pulse-amplitude modulation, and orthogonal frequency division multiplexing modulation formats are used to demonstrate the data transmission capabilities of

this LED array over free space, with error-free data transmission rates of 1.95, 2.37, and 4.81 Gb/s, respectively

Methodology

Water Sample Characterization:

The optical attenuation of light in natural waters is primarily caused by two primary wavelength-dependent processes, namely absorption and scattering, whose coefficients are indicated as $a()$ and $b()$, respectively, both with units of m^{-1} . According to a procedure frequently described in this work, clear tap water was treated with a mixture of aluminium and magnesium hydroxide (Maalox antacid) as a scattering agent to change the level of attenuation. The amount of scattering and consequent attenuation of the optical signal as it travels through the water increase as Maalox concentration rises. Although this method does not simulate effects like turbulence, it is an easy way to replicate various natural water analogues in a lab setting. Other organizations' thorough studies on the impact of turbulence.

The following measurements were made to determine how Maalox concentration and $c()$ related. Nine different Maalox concentrations, ranging from 0.000625% (1 ml of Maalox in 160 l of tap water) to 0.005625%, were looked at (9 ml of Maalox). A blue laser diode (Osram, PL450B) operating at the same nominal central wavelength as the LEDs (450 nm) was transmitted through the 1.5 m length of our water tank (dimensions 1.5 m 0.35 m 0.35 m) to determine $c()$ at each concentration. Since the divergence of the LED light would make it challenging to estimate $c()$, a laser was used for these observations. The laser diode's beam was collimated using a plastic aspheric lens (Thorlabs, CAY033) before being directed onto a power metre sensor (Thorlabs, S121C) situated on the opposite side of the tank. At each concentration, the received optical power, or PR, was measured. These PR values, Eq. (1), and the measured transmitted power of PT were used to calculate the corresponding attenuation coefficients for each water sample, which are displayed.

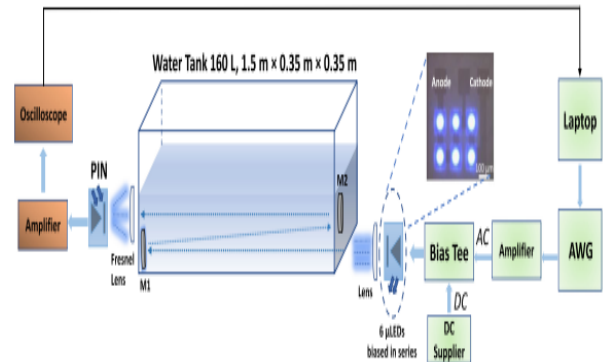


Fig 3: Water Sample Characterization

The characteristic of the following experiment is shown in figure:

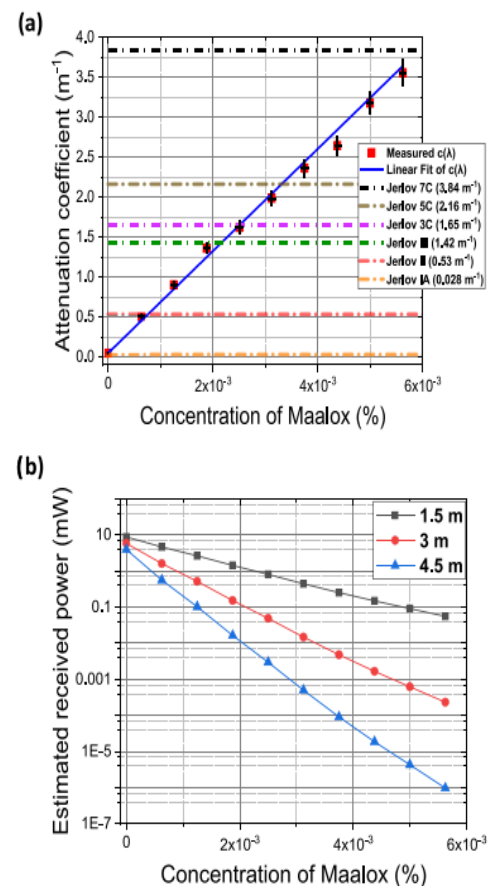


Fig 4: calculated

attenuation coefficients Vs content of scattering agent

Data Transmission and Experimental Set-Up:

The transmitted digital data signal was created and processed in MATLAB. This improved signal was then amplified and translated to analogue using an arbitrary waveform generator. To drive the LED arrays, the signal was mixed with a DC current of 30 mA through a bias tee.

The beam was collimated with a condenser lens so that it could be optically transmitted through the 1.5 m long water tank. Two 100 mm diameter mirrors (M1 and M2) were positioned properly in the tank to enhance the optical path up to 3 and 4.5 metres, respectively, for the longer-range data transfers. A 4-inch-diameter Fresnel lens was utilised to concentrate the collimated beam onto a PIN photoreceiver with a 1.4 GHz bandwidth at the receiver end. An amplifier was used to process the received signal, and an oscilloscope was used to record the results. Offline in MATLAB, the received signal was processed and demodulated. At this point, the received data and transmitted data are compared to find any improperly transmitted bits and calculate the BER.

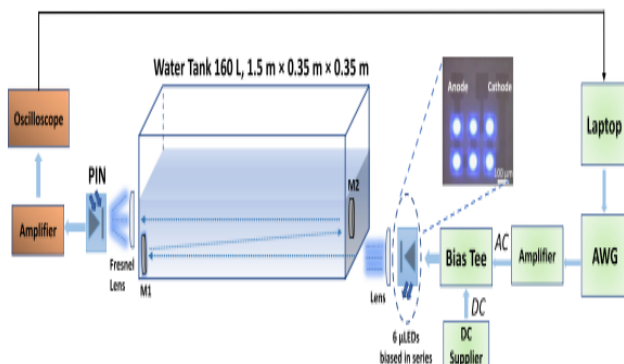


Fig 5: Experimental Setup

RESULTS

The measured BER using 60 mm-diameter series-connected LEDs as the transmitter and 1.5 m of clear water, while transmitting data at various data rates. The forward error correction (FEC) overhead of 7% of the gross data rate is the BER objective of 3.8×10^{-3} below which "error-free" data transmission can be accomplished. Although FEC was not actually employed in this work, the highest attainable data rate that satisfied this condition was 4.92 Gb/s, which corresponds to a net data rate of 4.58 Gb/s after FEC.

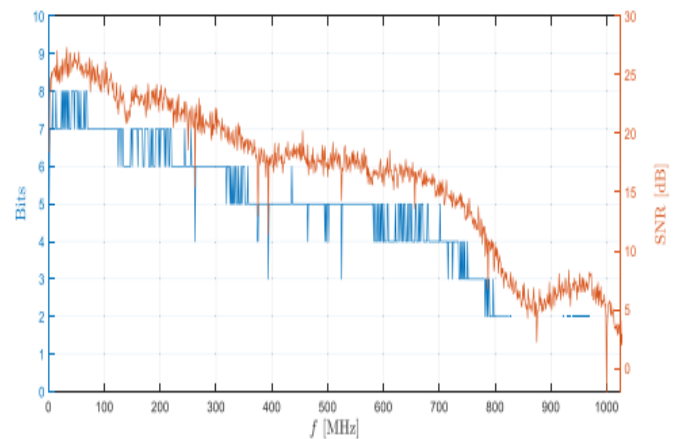


Fig 6: Measuring SNR and corresponding bit loading VS OFDM carrier frequency

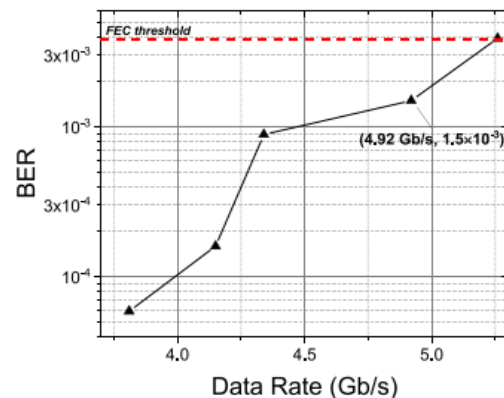


Fig 7: BER Vs Data rates for 60um LED in series

This graph displays the BER vs. data rates for the 80 mm series-connected LEDs over various water turbidities at a 1.5 m distance, as detailed in Section 3. It can be demonstrated that an increase in water turbidity results in attenuated transmission power levels that are captured by the detector and lower overall signal-to-noise ratios (SNR) levels. The maximum data rate through clear tap water is 3.78 Gb/s at a BER of 3.7×10^{-3} . Less information is loaded onto each subcarrier at a lower SNR level, which lowers the possible data rate. Extreme water turbidities ($c(450) = 3.56 \text{ m}^{-1}$) were used to demonstrate a data rate of up to 15 mb/s over 5.33 AIs.

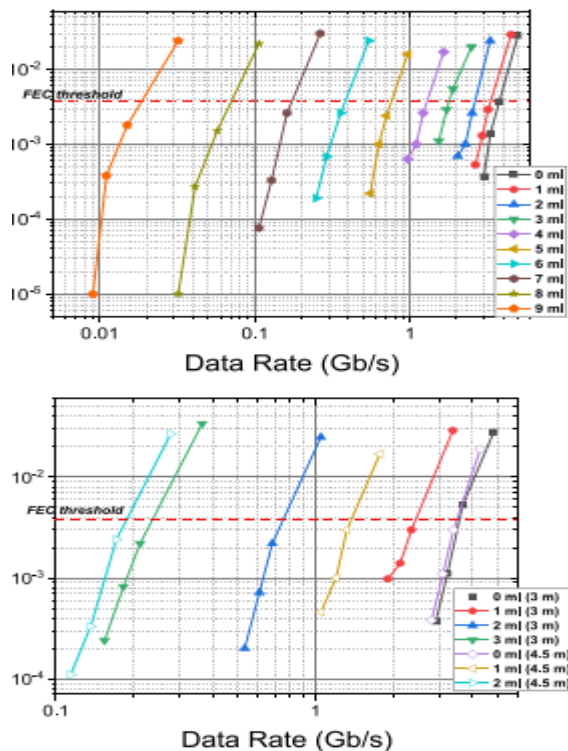


Fig 8 BER VS Data rates for 80um for different BERs.

This graph compares the maximum error-free data rates for all transmission distances to the quantity of ALs. For all path lengths, the maximum data rate falls as the number of ALs rises. This makes sense because

a lower SNR is produced by the signal's greater attenuation. The curves do not exactly overlap because each maximum data rate was obtained at a slightly different BER as shown, but it can be seen that similar data rates are obtained when the number of ALs is similar.

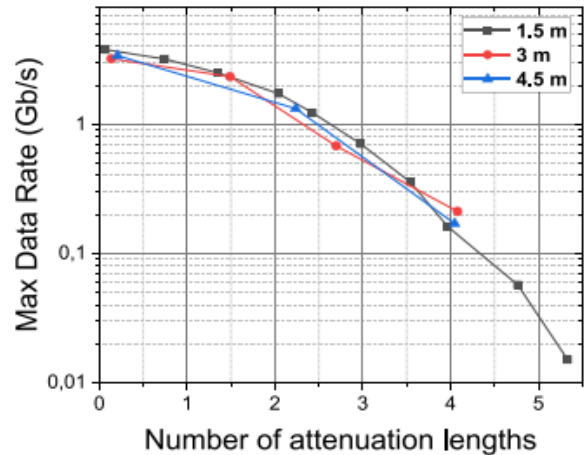


Fig 9: Max Data rates Vs No: of attenuation lengths

These findings suggest that even with turbid water samples, the relatively high power and bandwidth provided by series-connected LEDs can enable UWOC at Mb/s or Gb/s. Future research might increase the transmitting power by adding more LEDs, reduce the optical beam profile, or use multiplexing methods like wavelength division multiplexing to increase the achievable data rates and/or link lengths.

CONCLUSION

The effectiveness and precision of current summarization techniques are examined in this research. Using OFDM as the modulation scheme, Gb/s underwater optical wireless data transmissions over three underwater distances of 1.5 m, 3 m, and 4.5 m were made possible by the high output power and modulation bandwidth



of LED arrays, consisting respectively of 6 series-connected pixels of diameter 60 μ m or 80 μ m. For a maximum data rate of 4.92 Gb/s via 1.5 m of pure tap water with an attenuation coefficient of $c(450) = 0.05$ m⁻¹, a BER of 1.5×10^{-3} was attained. Additional underwater wireless optical transmissions were carried out through various levels of water turbidity. 2.34 Gb/s were shown for an attenuation coefficient of 0.5 m⁻¹, which is close to the Jerlov II open ocean type (0.53 m⁻¹), over 3 m, and 1.32 Gb/s were exhibited over 4.5 m. Using over 5.33 ALs and an attenuation coefficient of 3.56 m⁻¹, a data rate of 15 mb/s was accomplished via 1.5 m. We are currently looking into multi-wavelength operation for WDM, which is suitable with our strategy. The outcomes of this work demonstrate how series-connected LEDs may be used to enable high-speed underwater wireless communications despite various levels of water turbidity.

REFERENCES

[1] E. M. Sozer, M. Stojanovic, and J. G. Proakis, "Underwater acoustic networks," *IEEE J. Ocean. Eng.*, vol. 25, no. 1, pp. 72–83, Jan. 2000.

[2] P. Lacovara, "High-bandwidth underwater communications," *Marine Technol. Soc. J.*, vol. 42, no. 1, pp. 93–102, 2008.

[3] M. Stojanovic, "High-speed underwater acoustic communications," in *Underwater Acoustic Digital Signal Processing and Communication Systems*, Boston, MA, USA: Springer, 2013, pp.1-35

[4] C. Y. Li et al., "A 5 m/25 Gbps underwater wireless optical communication system," *IEEE Photon. J.*, vol. 10, no. 3, Jun. 2018, Art. no. 7904909.

[5] C. Uribe and W. Grote, "Radio communication model for underwater WSN," in *Proc. 3rd Int. Conf. New Technol. Mobility Secur.*, 2009, pp. 1–5.

[6] C. Y. Li et al., "A 5 m/25 Gbps underwater wireless optical communication system," *IEEE Photon. J.*, vol. 10, no. 3, Jun. 2018, Art. no. 7904909.

[7] C. Fei et al., "16.6 Gbps data rate for underwater wireless optical transmission with single laser diode achieved with discrete multi-tone and post nonlinear equalization," *Opt. Express*, vol. 26, no. 26, 2018, Art. no. 34060.

[8] R. X. G. Ferreira et al., "High bandwidth GaN-based micro-LEDs for multi-Gb/s visible light communications," *IEEE Photon. Technol. Lett.*, vol. 28, no. 19, pp. 2023–2026, Oct. 2016.

[9] P. Tian et al., "High-speed underwater optical wireless communication using a blue GaN-based micro-LED," *Opt. Express*, vol. 25, no. 2, pp. 1193–1201, 2017.

[10] E. Xie et al., "High-speed visible light communication based on a III-nitride series-biased micro-LED array," *J. Lightw. Technol.*, vol. 37, no. 4, pp. 1180–1186, Feb. 2019.